

Fluorescence Quenching of 1-Pyrenemethanol by Serotonin on the Surface of Polystyrene Latex Particles

Kenichi Nakashima,* Daigo Koide, and Yong-Kuan Gong

Department of Chemistry, Faculty of Science and Engineering, Saga University, 1 Honjo-machi, Saga 840-8502

(Received November 8, 1999)

The fluorescence quenching of 1-pyrenemethanol (PyM) by serotonin (Ser) in polystyrene latex dispersions has been studied by steady-state and time-resolved fluorescence spectroscopy. From steady state fluorescence measurements, it is found that the quenching is remarkably enhanced on going from an aqueous homogeneous solution to a latex dispersion. This is attributed to that both PyM and Ser are effectively adsorbed onto the latex particles, as evidenced by measurements of the adsorption isotherms. Fluorescence decay curves of PyM in polystyrene latex dispersions have been successfully analyzed in terms of double exponential functions. The analysis reveals that the quenching of PyM fluorescence by Ser on polystyrene latex surfaces is mainly operated by a static mechanism, although the contribution of a dynamic mechanism is not negligible.

Latex particles have been employed for the design of diagnostic reagents and drug-delivery systems in the field of biomedical science.^{1–4} This is due to the unique characteristics of the surface of latex particles. The surface consists of organic polymers embedded sparsely with functional groups, such as sulfate, carboxyl, or amino groups. It is possible to modify the latex surface to have the desired polarity (and thus desired hydrophilicity in aqueous media), because (1) various kinds of functional groups can be introduced onto the surfaces, (2) the concentration of the functional groups on latex surfaces can be easily controlled, and (3) different types of polymers, such as polystyrene and polyacrylates, with varying degrees of polarity can be employed as the support material. Accordingly, latex particles can provide biomedically important compounds (e.g. proteins) with various kinds of adsorption patterns on the surface. It is also possible to covalently bind some compounds to the functional groups on the latex surface. Furthermore, latex particles have other features, as follows: (4) the particle shape is highly uniform (spherical), and (5) the particles size can be controlled within a narrow distribution.

To extend the use of latex particles in the biomedical field, it is important to investigate the photoreactions of biologically important compounds on a latex surface. The importance of such investigations will be especially significant when latex particles are used for photodynamic therapy.

In this study, we investigated the electron transfer quenching of the fluorescence of 1-pyrenemethanol (PyM) by serotonin (Ser) on the surface of polystyrene (PS) latex particles. Ser is an analogue of tryptophan, and is known to act as a neurotransmitter in brains and a hemostatic compound in platelets. PyM can be regarded as a model compound of polynuclear aromatic hydrocarbons, some of which are carcinogenic. The present work was intended to reveal the photophysical and photochemical behaviors of biomedically

important compounds on the surface of latex particles. The obtained results will provide background information for the possible use of latex particles in biomedical science.

Experimental

PyM (Molecular Probes, Inc.) was used as received. Serotonin (Ser-HCl) from Tokyo Kasei Kogyo Co., Ltd. was of guaranteed grade, and was used without further purification. Water was purified with a Millipore Milli Q purification system.

Styrene monomer was washed with a 2% sodium hydroxide solution, followed by vacuum distillation. The PS latex was synthesized by standard emulsion polymerization in the presence of sodium dodecyl sulfate.⁵ The latex was repeatedly dialyzed against water until the conductivity of the serum was reduced to that of Milli Q water. The diameter of the latex particles was determined with an Otsuka ELS-800 dynamic light-scattering spectrophotometer. The mean diameter is 182 nm with a narrow size distribution.

Stock solutions of PyM and Ser in water were prepared to give concentrations of 10 μM ($1\text{ M} = 1\text{ mol dm}^{-3}$) and 10 mM, respectively. PyM was completely dissolved in water at a concentration of 10 μM . Portions of the PS dispersion and the stock solutions of the probes were mixed in a 10-mL ($1\text{ L} = 1\text{ dm}^3$) volumetric flask, followed by sonication for 5 min. The samples were stored in the dark for 1 d before conducting spectroscopic measurements. In fluorescence experiments, the samples were deaerated by nitrogen-purging for 15 min, unless otherwise mentioned.

Adsorption isotherms of PyM and Ser onto the latex surface were measured by ultracentrifugation. Portions of the latex dispersion containing known amounts of the probe were placed in ultracentrifuge tubes, and centrifuged with a Beckman Avanti-30 ultracentrifuge for 60 min at 26×10^3 rpm ($57 \times 10^3 g$). The concentration of the probe in the supernatant after centrifugation was determined by UV absorption. The amount of the probe adsorbed was calculated from the difference of the total concentration in the dispersion and equilibrium concentration in the serum.

Fluorescence spectra were recorded on a Hitachi F-4000 spectrofluorometer. The spectra were corrected by the use of a standard

tungsten lamp with a known color temperature. The steady-state fluorescence intensity of PyM is expressed in terms of the peak height of a band around 395 nm, unless otherwise stated. The absorption spectra were measured with a JASCO Ubest-50 spectrophotometer. Fluorescence decay curve measurements were performed with a Horiba NAES 1100 time-resolved spectrofluorometer that uses a time-correlated single photon counting technique. In the measurements of the fluorescence decay curves, the excitation light from a hydrogen lamp was monochromated through a grating monochromator. Furthermore, a band-pass filter (Hoya U340) was placed between the excitation monochromator and the sample. By setting the band-pass filter, it was possible to greatly reduce any stray-light which introduces strong scattering light into the detector in the case of latex samples. The fluorescence emission from the sample was collected through a sharp-cut filter (Hoya L37) to remove the excitation light.

Results and Discussion

Steady-State Fluorescence Study. We observed the fluorescence spectra of PyM in both the absence and presence of Ser (Fig. 1). It is known that the fluorescence of pyrene and its derivatives is quenched by indolic compounds through electron transfer.^{6–10} As can be seen from Fig. 1, the fluorescence of PyM is markedly quenched by Ser on going from an aqueous homogeneous solution to a PS latex dispersion. It is noted that quenching in the latex dispersion is effectively brought about even when the Ser concentration is lowered to 2 μM , which is several hundreds of times smaller than that needed for quenching in aqueous solutions. The marked enhancement of quenching can be ascribed to an increase in the local concentrations of PyM and Ser on the latex surface, as confirmed by measurements of the adsorption isotherms (data shown later). The Ser employed was in a form of hydrochloride, and the pH of the aqueous solution was around 6 over the concentration range shown in Fig. 1b. At this pH, Ser exists almost in a cationic form. Thus, electrostatic attraction between Ser and sulfate groups on the latex surface seems to play the main role in Ser adsorption. On the other hand, PyM seems to be adsorbed onto the latex surface by a hydrophobic interaction between PyM and the PS matrix.

In Fig. 2, we plot the PyM fluorescence intensity against the Ser concentration in an aqueous homogeneous solution and a PS latex dispersion. The plot for the aqueous solution is linear, giving a Stern–Volmer constant of 507 M^{-1} . Using lifetime data ($\tau_f = 190 \text{ ns}$) obtained by us earlier,¹¹ we calculated the quenching rate constant for an aqueous solution: $k_q = 2.7 \times 10^9 \text{ M}^{-1} \text{ s}^{-1}$. This value is close to that ($k_q = 2.4 \times 10^9 \text{ M}^{-1} \text{ s}^{-1}$) for a PyM–tryptophan pair in an aqueous solution.¹²

In contrast to the plot for the aqueous solution, the plot for the latex dispersion shows a downward curve. Such downward-curving plots were investigated by Eftink and Ghiron^{13,14} for various cases. According to them, a downward curving plot is obtained when a fluorophore is distributed in two or more different environments which have different accessibility to fluorescence quenching (*heterogeneously emitting system*). Instead of the general

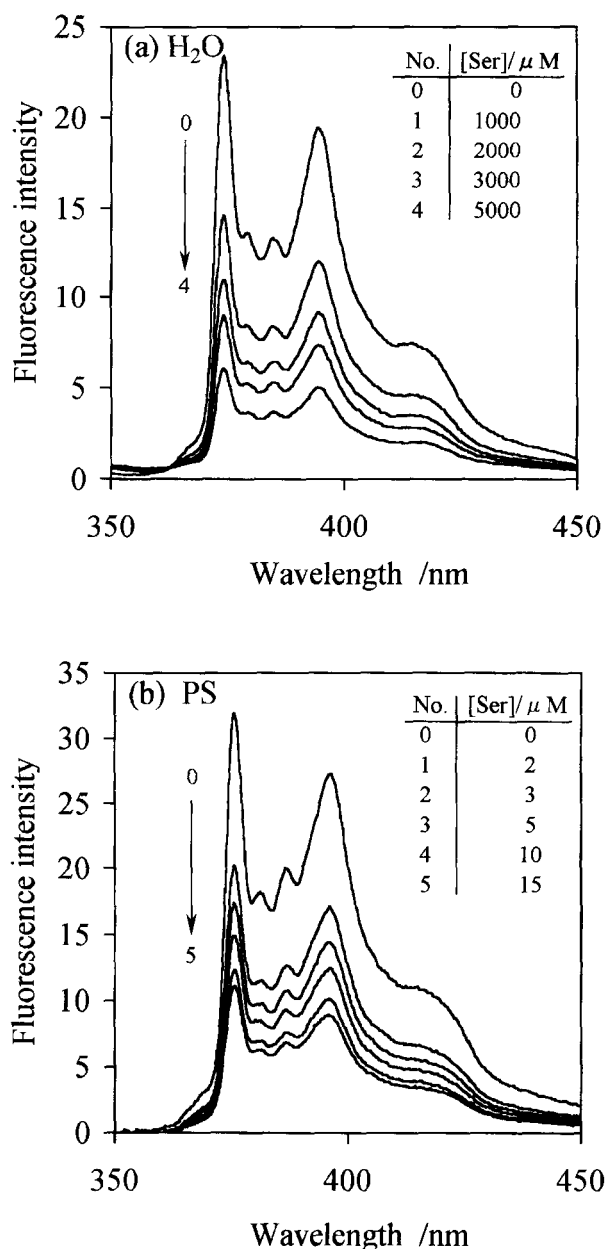


Fig. 1. Fluorescence spectra of PyM in the absence and presence of Ser. (a) Aqueous solution: $[\text{PyM}] = 1.0 \mu\text{M}$; (b) PS latex dispersion: $[\text{PyM}] = 1.0 \mu\text{M}$, $[\text{PS}] = 1.15 \text{ g dm}^{-3}$. The samples are excited at 340 nm. Excitation and emission bandpasses are 5 and 1.5 nm, respectively. The spectra for PS latex dispersions are corrected for the back ground scattering of excitation light.

treatment of the heterogeneously emitting system, we employ here a simplified treatment,¹⁵ because the former treatment contains many parameters to be determined. We assume two locations of a fluorophore: one is accessible to the quencher (denoted as *a*) and the other is inaccessible (*b*). A quantitative expression for the relation between the fluorescence intensity and the quencher concentration ($[Q]$) is given by

$$I_0/(I_0 - I) = 1/f_a K_a [Q] + 1/f_a, \quad (1)$$

$$f_a = I_{0a}/(I_{0a} + I_{0b}) = I_{0a}/I_0, \quad (2)$$

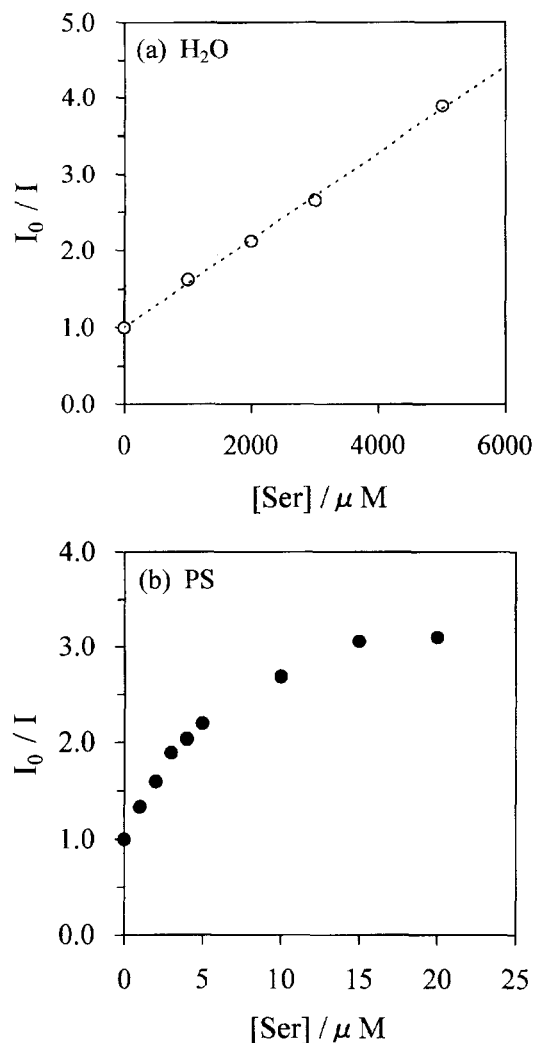


Fig. 2. Stern-Volmer plots for the systems in Fig. 1. (a) Aqueous solution; (b) PS latex dispersion. In Fig. 2b, several data are added to those in Fig. 1b.

where I_0 and I denote the total fluorescence intensities of the fluorophore in the absence and presence of the quencher, respectively.¹⁵ I_{0i} ($i = a, b$) represents the contribution to I_0 from the component in environment i . K_a is a quenching constant for the fluorescent component in environment a .

We plot $I_0/(I_0 - I)$ against $1/[\text{Ser}]$ in Fig. 3, where the total concentration of Ser in the latex dispersion is employed instead of the local concentration on the latex surface, because it is difficult to estimate the local concentration of the quencher, which is probably distributed two-dimensionally on the latex surface. The plot in Fig. 3 shows a good linearity between $I_0/(I_0 - I)$ and $1/[\text{Ser}]$, although the treatment is too simplified. From the intercept and slope, we obtain $f_a = 0.76$ and $K_a = 4.9 \times 10^5 \text{ M}^{-1}$. The value of f_a (0.76) suggests that about 76% of PyM molecules are located at the environment which is accessible to the quenching.

It is interesting for us to obtain insights into environments a and b for substantiating the above analysis. The accessible environment a is probably the surface of the latex particles, which is exposed to water. As for the inaccessible site b ,

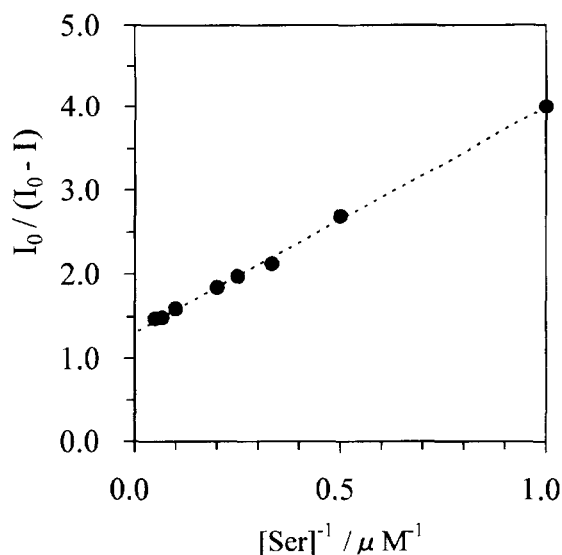


Fig. 3. Modified Stern-Volmer plot for the systems in Fig. 2b.

there seems to be two possibilities: (1) some kinds of hole inside the latex particles, which PyM can diffuse in but Ser cannot, and (2) an aqueous phase where the quenching of PyM fluorescence by Ser is inefficient at such low concentrations as several μM . We first consider case 2. In this case, the population of PyM on the latex surface should be close to f_a ($= 0.76$). To obtain the population of PyM on the latex surface, we observed an adsorption isotherm (Fig. 4a). The horizontal axis of Fig. 4a represents the total concentration of PyM in the latex dispersion, and the vertical axis represents the concentration of adsorbed PyM, which is calculated as the difference between the total concentration in the dispersion and the equilibrium concentration in the supernatant. Accordingly, the slope of the line in Fig. 4a gives the mole fraction of PyM on the latex particles. It can be seen from Fig. 4a that 85% of PyM exists on the latex particles. This value (0.85) is larger than the value of f_a (0.76). This difference may be partly originated from the roughness of the treatment yielding Eq. 1. As another reason for the difference, we take the case 1 into account. In contrast to PyM, which is hydrophobic, Ser molecules are almost in a cationic form under the experimental condition. If there is some hydrophobic hole in the latex particles, PyM can diffuse in the hole, but Ser cannot. In this situation, PyM molecules in the hole are not accessible to quenching, despite the fact that they are adsorbed onto the latex particles. In conclusion, both of cases 1 and 2 seem to be needed to explain the inaccessible site b .

We present an adsorption isotherm of Ser onto the latex particles in Fig. 4b, where the total concentration of Ser is varied over the same range as in Fig. 2b. As we can see, the adsorption isotherm is downward curving. This indicates that the adsorption coefficient of Ser decreases with increasing total concentration, so that the local concentration of Ser on the latex surface does not linearly increase with the total concentration. Therefore, the downward-curving nature in Stern-Volmer plot for the latex systems (Fig. 2b) seems to be

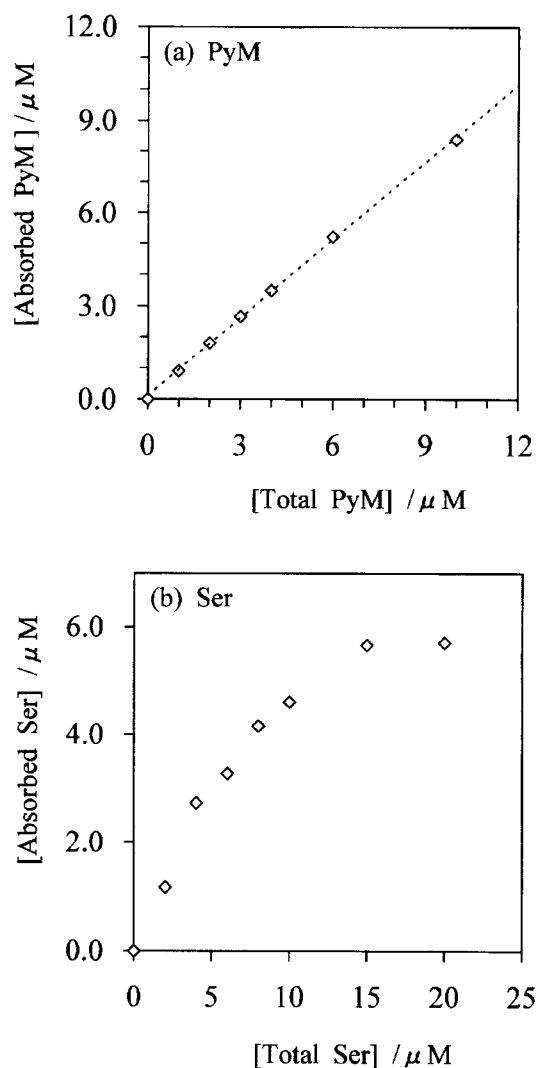


Fig. 4. Adsorption isotherms of (a) PyM and (b) Ser onto PS latex particles at 20 °C. $[PS] = 1.15 \text{ g dm}^{-3}$. The horizontal axis represents the total concentration of the probe in the latex dispersion, and vertical axis does the concentration of adsorbed probe. Accordingly, the slope of the line gives the mole fraction of the probe adsorbed on the latex particles.

ascribed, in part, to this adsorption behavior of Ser. However, if we compare Fig. 4b with Fig. 2b, we note that the profiles of the two downward curves are not the same. Therefore, both the heterogeneously emitting PyM and the adsorption behavior of Ser seem to be responsible for the downward-deviation of the Stern–Volmer plot.

Time-Resolved Fluorescence Study. To obtain insight into the mechanism of quenching of PyM fluorescence by Ser, we observed the fluorescence decay curves of PyM in both the absence and presence of Ser (Fig. 5). It turned out that the decay curves of PyM in the latex dispersion conform to a double-exponential function, even when Ser is absent,

$$I(t) = A_1 \exp(-t/\tau_1) + A_2 \exp(-t/\tau_2), \quad (3)$$

where τ_1 and τ_2 denote the lifetime of each component, and A_1 and A_2 are pre-exponential factors. Here, it is of value

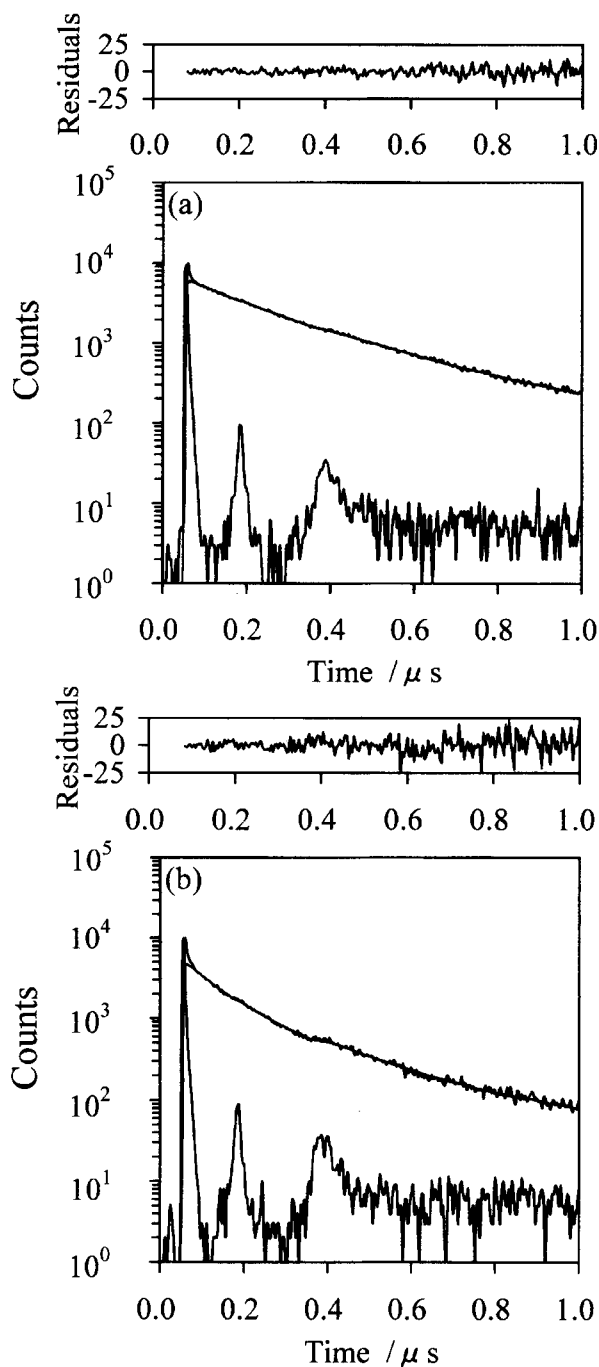


Fig. 5. Fluorescence decay curves of PyM in PS latex dispersions: (a) in the absence of Ser, (b) in the presence of Ser (20 μM). $[PyM] = 1.0 \text{ μM}$, $[PS] = 1.15 \text{ g dm}^{-3}$. The samples are excited at 325 nm and the excitation bandpass is 14 nm. The emission is collected through a cut-off filter (Hoya L37). A band-pass filter (Hoya U340) was put between the excitation monochromator and the sample to reduce a stray-light.

to note that the integration of each term in Eq. 3 with respect to time (t) gives a relative quantum yield (y_i) of the corresponding component,

$$y_i = \int A_i \exp(-t/\tau_i) dt = A_i \tau_i. \quad (\text{for } i = 1, 2) \quad (4)$$

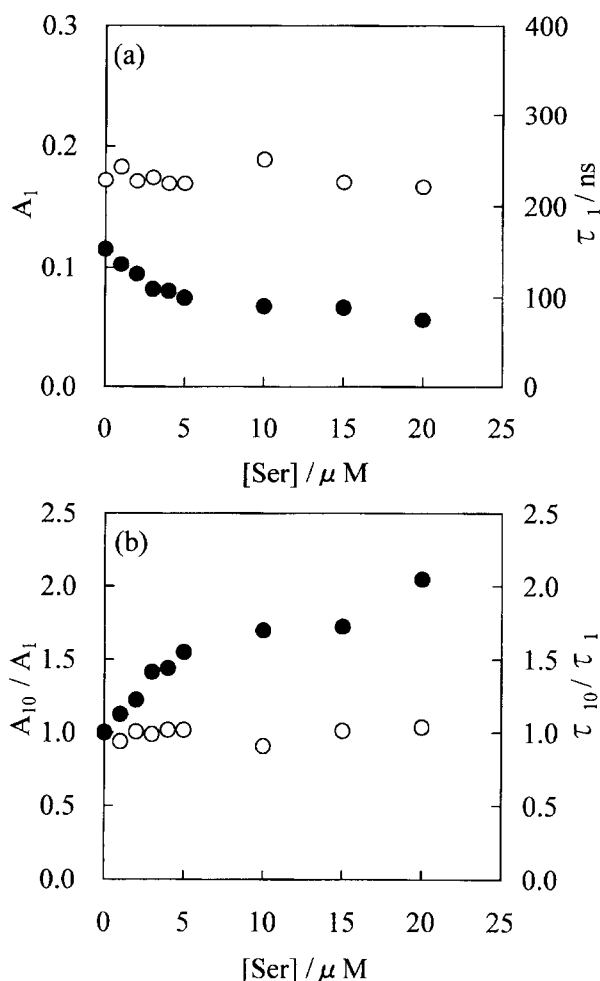


Fig. 6. (a) Lifetime (●) and pre-exponential factor (○) of the component 1 of PyM fluorescence as a function of the concentration of Ser in a PS latex dispersion. (b) Stern–Volmer plots for A_1 and τ_1 . [PyM] = 1.0 μM , [PS] = 1.15 g dm^{-3} .

For the convenience of a later discussion, we define the total quantum yield (Y) as

$$Y = y_1 + y_2 = A_1 \tau_1 + A_2 \tau_2. \quad (5)$$

We obtained from Fig. 5a $\tau_1 = 154$ ns ($A_1 = 0.172$) and $\tau_2 = 297$ ns ($A_2 = 0.149$). The two-component nature of the decay curve seems to be ascribed to that PyM is partitioned in two different milieus: one (τ_1) is roughly assignable to the species in an aqueous phase and the other (τ_2) to those on the latex particle. The shorter component, however, seems to contain a contribution from the scattered excitation light, since the value of τ_1 is less than that obtained for an aqueous solution. It is also probable that the shorter component contains a contribution from the species on the latex particles because τ_1 is increased as the concentration of the latex particles is increased from 0 to 0.1 g L^{-1} , and becomes constant after that (data not shown).

An analysis of the decay component is quite useful for obtaining information about whether the quenching is *dynamic* or *static*.^{16,17} In dynamic quenching, τ_i is decreased with increasing quencher concentration, while A_i is not changed, as

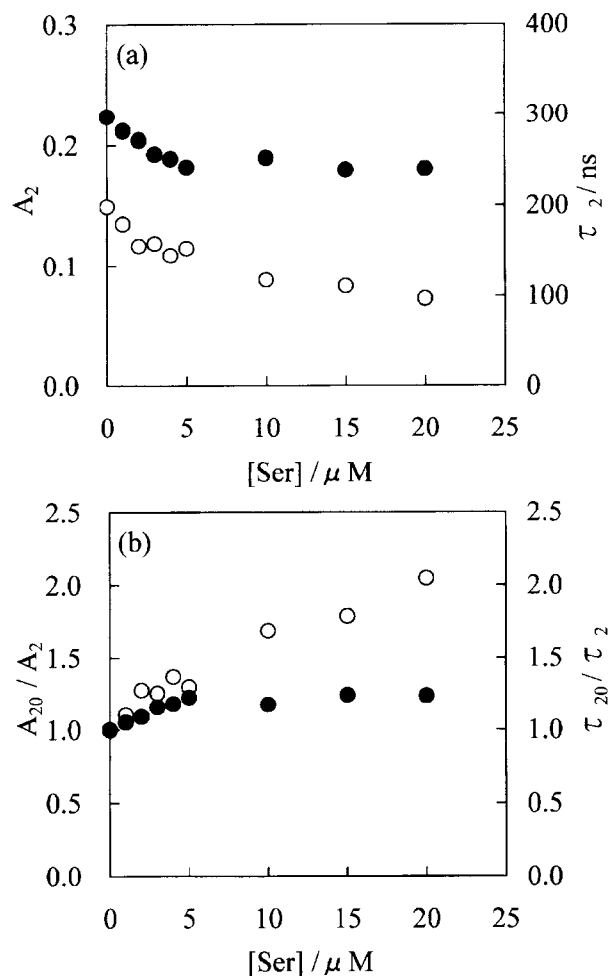


Fig. 7. As in Fig. 6, but for the component 2.

can be seen from the well-known Stern–Volmer equation:

$$y_{i0}/y_i = A_{i0} \tau_{i0}/A_i \tau_i = \tau_{i0}/\tau_i = 1 + K_D[Q], \quad (6a)$$

$$A_{i0}/A_i = 1, \quad (6b)$$

where the subscript 0 means the absence of a quencher.^{16,17} In static quenching, on the other hand, A_i is decreased with increasing quencher concentration, while τ_i remains constant:

$$y_{i0}/y_i = A_{i0} \tau_{i0}/A_i \tau_i = A_{i0}/A_i = 1 + K_S[Q], \quad (7a)$$

$$\tau_{i0}/\tau_i = 1. \quad (7b)$$

We plot A_1 , τ_1 , and A_{10}/A_1 as a function of the Ser concentration in Fig. 6. A_2 , τ_2 , and A_{20}/A_2 are also plotted in Fig. 7. As can be seen from Fig. 6, the A_1 value is almost constant when the Ser concentration is increased from 0 to 20 μM , whereas τ_1 is significantly decreased (from 154 to 75.3 ns). The small change in A_1 and the significant change in τ_1 suggest that the quenching of component 1 is mainly operated by a dynamic mechanism, although the Stern–Volmer plot for τ_1 is not linear. The dynamic-quenching nature of the component 1 is consistent with our former conclusion that this component can be roughly assigned to the fraction of PyM in an aqueous phase.

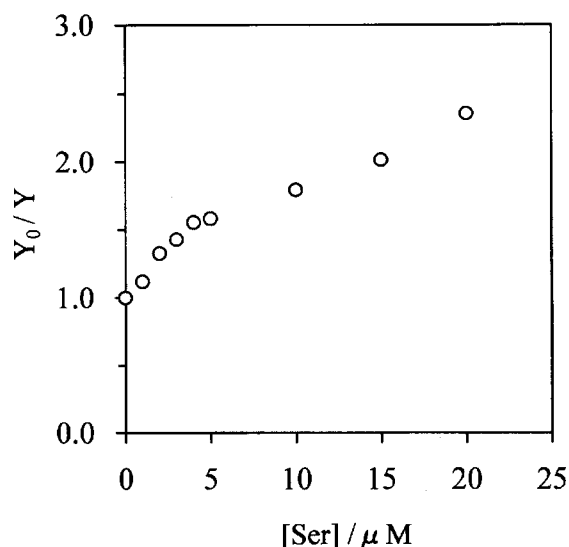


Fig. 8. Plot of Y_0/Y vs. $[\text{Ser}]$ obtained from time-resolved fluorescence measurements for the same systems as in Fig. 2b. Y_0 and Y are the total fluorescence quantum yields of PyM in the absence and presence of Ser, respectively (see Eq. 5).

In contrast to component 1, both the pre-exponential factor and the lifetime of component 2 show significant changes when the quencher concentration is varied from 0 to 20 μM (Fig. 7). Thus, the quenching of component 2 seems to be explained by a combined dynamic and static mechanism.¹⁷ If we compare the Stern–Volmer plot for A_2 with that for τ_2 , however, we realize that the change in A_2 is much larger than that in τ_2 . Therefore, we conclude that quenching of the component is dominated by a static mechanism.

It should be noted here that components 1 and 2 in the decay curve do not simply correspond to components a and b in the modified Stern–Volmer equation (Eq. 1) for the steady-state fluorescence data. This is obvious from the fact that both components 1 and 2 are subjected to quenching, whereas component b is supposed to be free from quenching. As stated, the two-site quenching model shown by Eq. 1 is too simplified. Therefore, it is difficult to find a one-to-one correspondence between them.

In Fig. 8, we plot Y_0/Y against the concentration of Ser. As Y_0 and Y are the total quantum yields of PyM fluorescence in both the absence and presence of the quencher, respectively, the plot in Fig. 8 corresponds to that in Fig. 2b. It is of note that I_0/I (Fig. 2b) and Y_0/Y (Fig. 8) show a similar dependence on the quencher concentration, although the former is obtained from steady-state fluorescence measurements, while the latter from time-resolved experiments. This similarity assures the reliability of the present two measurements.

Conclusions

We have shown from steady state fluorescence measurements that the quenching of PyM fluorescence by Ser is about several hundred times enhanced upon going from the aqueous homogeneous solution to the PS latex dispersion. This is attributed to an increase in the local concentrations of both

PyM and Ser on the latex surface, as evidenced by the measurements of the adsorption isotherms. The Stern–Volmer plot for PyM–Ser in the aqueous solution is linear, giving a quenching rate constant of $2.7 \times 10^9 \text{ M}^{-1} \text{ s}^{-1}$, while the plot for the same pair in the latex dispersion becomes downward-curving. The downward curve seems to be explained, in part, by a model of a *heterogeneously emitting system*,^{13–15} which assumes the distribution of a fluorophore in two environments: one is accessible to quenching and the other is not. The deviation of the Stern–Volmer plot from linearity is also ascribed to the change in the adsorption coefficient of Ser onto the latex particles.

The mechanism of the fluorescence quenching in the latex dispersion has been investigated by time-resolved fluorescence measurements. The fluorescence decay curve of PyM shows a double-exponential nature in the latex dispersion, suggesting the distribution of this fluorophore in two different milieus: One is roughly assignable to an aqueous phase and the other to the surface of latex particles. From the dependence of the decay profiles of PyM fluorescence on the Ser concentration, it is elucidated that the quenching on the latex surface is mainly operated by a static mechanism, although the contribution of a dynamic mechanism is not negligible.^{16,17}

The present work is partly defrayed by the Grant-in-Aid for Scientific Research on Priority-Area-Research “Photoreaction Dynamics” No. 08218249 from the Ministry of Education, Science, Sports and Culture.

References

- 1 L. Quali, E. Pefferkorn, A. Elaissari, C. Pichot, and B. Mandrand, *J. Colloid Interface Sci.*, **171**, 276 (1995).
- 2 D. Kowalczyk and S. Slomkowski, *J. Bioact. Compat. Polym.*, **9**, 282 (1994).
- 3 S. Slomkowski and T. Basinska, in “Polymer Latexes,” ed by E. S. Daniels, E. D. Sudol, and M. S. El-Aasser, ACS Symp. Ser. 492, Washington, DC (1992), p. 328.
- 4 T. Suzawa, H. Shirahama, and T. Fujimoto, *J. Colloid Interface Sci.*, **86**, 144 (1982).
- 5 K. Nakashima, J. Duhamel, and M. A. Winnik, *J. Phys. Chem.*, **97**, 10702 (1993).
- 6 J. P. Palmans, M. Van der Auweraer, A. M. Swinnen, and F. C. De Schryver, *J. Am. Chem. Soc.*, **106**, 7721 (1984).
- 7 M. V. Encinas and E. A. Lissi, *Photochem. Photobiol.*, **44**, 579 (1986).
- 8 O. E. Zimerman, J. J. Cosa, and C. M. Previtali, *Photochem. Photobiol.*, **52**, 711 (1990).
- 9 H. A. Montejano, J. J. Cosa, H. A. Garrera, and C. M. Previtali, *J. Photochem. Photobiol. A: Chem.*, **86**, 115 (1995).
- 10 C. D. Borsarelli, H. A. Montejano, J. J. Cosa, and C. M. Previtali, *J. Photochem. Photobiol. A: Chem.*, **91**, 13 (1995).
- 11 K. Nakashima and N. Kido, *Photochem. Photobiol.*, **64**, 296 (1996).
- 12 K. Nakashima, S. Tanida, T. Miyamoto, and S. Hashimoto, *J. Photochem. Photobiol. A: Chem.*, **117**, 111 (1998).
- 13 M. R. Eftink and C. A. Ghiron, *Biochemistry*, **15**, 672 (1976).
- 14 M. R. Eftink and C. A. Ghiron, *Anal. Biochem.*, **114**, 199

(1981).

15 S. S. Lehrer, *Biochemistry*, **10**, 3254 (1971).

16 J. B. Birks, "Photophysics of Aromatic Molecules,"

Wiley-Interscience, London (1970).

17 J. R. Lakowicz, "Principles of Fluorescence Spectroscopy,"

Plenum Press, New York (1986).
